also that the corrected Pu^{240} distribution still differs significantly from that for the induced-fission case. In particular, in the mass region 132–140, the Pu^{240} distribution is much higher than the one for induced fission. From Fig. 5 this is also the region where the largest amount of kinetic energy is released.

The amount of Pu^{240} in the sample was calculated by using the α-decay rate obtained after correction for contributions from other plutonium isotopes and Am^{241} (produced by the decay of Pu^{241}). The Pu^{240} spontaneous-fission rate calculated by using this value was 2.5 fissions/h, while the measured rate was 2.16 fissions/h. If Cf^{252} was present in significant amounts, the measured α-decay rate should change negligibly, but the fission rate should be 50% higher than the calculated one. This is another indication that the Cf^{252} contamination is negligible.

The above analysis leads us to believe that the observed structures in the mass and kinetic energy distributions were not produced by any contamination but are the true characteristics of the spontaneous fission of Pu^{240}.

†Work supported by the U.S. Atomic Energy Commission.

[1]W. J. Whitehouse and W. Galbraith, Phil. Mag. 41, 429 (1950).

[2]E. Segre and C. Wiegand, Phys. Rev. 94, 157 (1954).

[3]T. A. Mostovaya, in *Proceedings of the Second United Nations International Conference on the Peaceful Uses of Atomic Energy* (United Nations, Geneva, Switzerland, 1958), Vol. 15.

[4]V. N. Okolovich and G. N. Smirenkin, Zh. Eksperim. i Teor. Fiz. 43, 1861 (1962) [transl.: Soviet Phys.-JETP 16, 1313 (1963)].

[5]A. Smith, P. Fields, A. Friedman, S. Cox, and R. Sjoblom, in *Proceedings of the Second United Nations International Conference on the Peaceful Uses of Atomic Energy* (United Nations, Geneva, Switzerland, 1958), Vol. 15.

[6]J. B. Laidler and F. Brown, J. Inorg. Nucl. Chem. 24, 1485 (1962).

[7]J. Toraskar and E. Melkonian, Phys. Rev. C 4, 267 (1971).

[8]H. W. Schmitt, J. H. Neiler, and F. J. Walter, Phys. Rev. 141, 1146 (1966).

[9]B. C. Diven and J. C. Hopkins, in *Proceedings of the Seminar on the Physics of Fast and Intermediate Reactors, Vienna, Austria, 1961* (International Atomic Energy Agency, Vienna, Austria, 1962) Vol. 1, p. 149.

PHYSICAL REVIEW C VOLUME 4, NUMBER 4 OCTOBER 1971

Neutron-Hole-State Structure in $N = 81$ Nuclei. II. ^{140}Ce and ^{138}Ba(p, d)†

R. K. Jolly and E. Kashy

Cyclotron Laboratory, Michigan State University, East Lansing, Michigan 48823

(Received 5 May 1971)

In continuation of our program of neutron-hole-state studies in $N = 81$ nuclei, angular distributions of deuterons from (p,d) reactions (energy resolution ~35 keV) on ^{140}Ce and ^{138}Ba at $E_p = 35$ MeV have been measured and compared with distorted-wave Born-approximation calculations including finite-range and nonlocality corrections. These calculations yield acceptable spectroscopic factors and are in fair agreement with the shapes of the experimental angular distributions. The neutron-single-hole energies have been determined. These energies (in MeV) are $d_{3/2}$, 0.0; $s_{1/2}$, 0.33; $h_{11/2}$, 1.07; $d_{5/2}$, 1.72; and $g_{7/2}$, 2.90 for ^{139}Ce; and $d_{3/2}$, 0.0; $s_{1/2}$, 0.54; $h_{11/2}$, 1.07; $d_{5/2}$, 1.71; and $g_{7/2}$, 2.93 for ^{137}Ba.

Considerable fractionation of the $(2d_{5/2})_\nu^{-1}$ and the $(1g_{7/2})_\nu^{-1}$ states is observed while the $(1h_{11/2})_\nu^{-1}$ and the $(3s_{1/2})_\nu^{-1}$ states are each observed to split mostly into two components. Systematics of the energies and strengths of the various neutron-single-hole states and their components are presented for all $N = 81$ nuclei from ^{137}Ba through ^{143}Sm and the significance of the systematics discussed. No measurable population of any neutron state in the $82 < N \leq 126$ major shell has been observed.

I. INTRODUCTION

In a previous paper[1] (henceforth referred to as Paper I) we reported our results on the analysis of (p, d) measurements on the $N = 82$ nuclei of ^{144}Sm and ^{142}Nd[1] together with a study of the effects of different values of lower cutoff, finite-range and nonlocality (FRNL) corrections, and density dependence of the effective pn interaction on the shapes and magnitudes of distorted-wave Born-approxima-

tion (DWBA) cross sections. In the present paper we report our results from (p, d) measurements made on ^{140}Ce and ^{138}Ba. These results along with those presented in Ref. 1 constitute a sufficiently large sample of data on the $N=81$ nuclei to provide detailed information on the strengths, energies, splitting, and movement of the single-neutron-hole states as a function of the valence proton number $(Z-50)$ in these nuclei. The valence protons in these nuclei are filling the same shell-model orbits (i.e., $1g_{7/2}$, $2d_{5/2}$, $1h_{11/2}$, $3s_{1/2}$, and $2d_{3/2}$) as the neutrons in the $50<N\leq 80$ range so that the pn interaction between them can cause observable changes in the splitting and energies of neutron-single-hole states as a function of changes in Z. Such effects have been investicated by Yagi[2] in the nuclei of ^{139}Ce, ^{117}Sn, and ^{91}Zr, and his findings have been compared with ours in Sec. IV.

In the following section we very briefly describe some details of the experimental arrangement and the DWBA calculations used in the present analyses, as these aspects of the present work have been discussed in some detail in Paper I. Sec. III describes the results of the spectroscopy of ^{139}Ce and ^{137}Ba and their comparison with results from other measurements. In Sec. IV we present the combined results of Paper I and the present paper on various aspects of neutron-hole states in ^{143}Sm, ^{141}Nd (from Paper I), ^{139}Ce, and ^{137}Ba along with a discussion of the significance of these data.

II. DATA ACQUISITION AND ANALYSIS

A. Experimental Procedure

35-MeV protons from the Michigan State University variable-energy cyclotron were used to bombard isotopic targets of ^{140}Ce and ^{138}Ba [see Table I for target and (p, d) Q-value[3] data], and the reaction products were analyzed with a ΔE-E counter telescope arrangement optimized to yield ~35-keV energy resolution. Energy spectra for up to 2.2 MeV of excitation energy in the residual nucleus were also measured at 20° with position sensitive detectors in the focal plane of our Enge split-pole spectrograph (energy resolution 10–15 keV) to resolve any multiplets seen in the counter telescope spectra. The reader is referred to Paper I for details of target preparation and data acquisition.

TABLE I. Target composition and $Q(p, d)$ values.

Target	Chemical formula	Enrichment (%)	$Q(p, d)$ [a] (MeV)
^{140}Ce	CeO_2	99.7	6.814 ± 0.052
^{138}Ba	$Ba(NO_3)_2$	99.8	6.317 ± 0.086

[a] Taken from Ref. 3.

Absolute (p, d) cross sections were obtained by simultaneously measuring the (p, p) and (p, d) spectra at 30, 40, and 50°, and fitting these limited elastic scattering angular distributions to the optical-model predictions using the same parameters as in the DWBA calculations described below. The uncertainty in this normalization procedure is estimated at ≲10%.

B. DWBA Calculations

To extract spectroscopic information from the experimental angular distributions, DWBA calculations were performed using the Oak Ridge National Laboratory code JULIE.[4] The proton optical-model parameters were the fixed-geometry average parameters of Perey.[5] Similarly the deuteron parameters used were the fixed-geometry parameters of Perey and Perey.[6] It was shown in Paper I that the DWBA calculations including FRNL corrections yield good shape agreement with the experimental angular distributions and acceptable spectroscopic factors. Consequently only FRNL DWBA calculations were compared with the normalized experimental angular distributions in the present work. The various parameters used in these calculations are listed in Table II (see also Refs. 7 and 8).

The spectroscopic factors were calculated using the equation[4]

$$\sigma_{\text{expt}}(\theta) = \tfrac{3}{2} D_0^2 S \sigma_{\text{DWBA}}(\theta), \tag{1}$$

where D_0 is the overlap integral discussed in Paper I and S is the spectroscopic factor. Only $T_<$ states were observed so that the sum rule for the spectroscopic factors measured here is[9]

$$S_<^{Nlj} = \nu^{Nlj} - \frac{\pi^{Nlj}}{2T+1}, \tag{2}$$

TABLE II. Optical-model parameters for protons (Ref. 5) and deuterons (Ref. 6) used in the present calculations. The symbols used have their usual meaning (see Refs. 5 and 6, if necessary). All lengths are in fermis and all well depths in MeV. The nonlocality parameters were taken from Refs. 7 and 8.

Protons ($E=35$ MeV)				Deuterons ($E\sim 25$ MeV)		
Nuclide	V_S	W_D	V_{so}	Nuclide	V_S	W_D
^{140}Ce	43.2	13.7	8.5	^{139}Ce	97.5	17.0
^{138}Ba	43.5	14.5	8.5	^{137}Ba	97.5	17.0
Fixed-geometry parameters				Fixed-geometry parameters		
$r_{0I}=r_{0S}=r_C=1.25$				$r_{0S}=r_{0C}=1.15$,		
$A_S=0.65$, $A_I=0.47$				$r_{0I}=1.34$		
				$A_S=0.81$, $A_I=0.68$		
Nonlocality parameters				Nonlocality parameters		
$\beta=0.85$ F (Ref. 7)				$\beta=0.54$ F (Ref. 8)		

where π^{Nlj} and ν^{Nlj} are the numbers of neutrons and protons occupying the same shell-model orbitals Nlj. The DWBA calculations were performed for the $2d_{3/2}$, $3s_{1/2}$, $1h_{11/2}$, $2d_{5/2}$, and $1g_{7/2}$ orbitals. With the exception of the $(2d_{3/2})_\nu^{-1}$ state, all the other neutron-hole states observed in the present work are split into several components. The energy centroids of these components were calculated as average energies weighted by the spectroscopic factors of the various components, i.e.,

$$\bar{E}_{Nlj} = \frac{(\sum_i S_i E_i)_{Nlj}}{(\sum_i S_i)_{Nlj}} . \quad (3)$$

Values of these energies and the total neutron-hole strength they correspond to in the nuclei of ^{139}Ce and ^{137}Ba shall be presented in the following section.

III. RESULTS AND DISCUSSION

A. ^{140}Ce$(p, d)^{139}$Ce

A sample energy spectrum from this reaction is shown in the top part of Fig. 1. A striking feature of the spectrum is the strongly excited low-lying states, the first four of which are the dominant components of the $(2d_{3/2})_\nu^{-1}$, $(3s_{1/2})_\nu^{-1}$, $(1h_{11/2})_\nu^{-1}$, and $(2d_{5/2})_\nu^{-1}$ states.

Angular distributions of these and several other states seen in the ^{140}Ce(p, d) reaction have been measured from 15 to 90°. These are shown in Figs. 2–5 where the data have been compared with FRNL DWBA calculations shown as broken or solid curves (exception 0.26-MeV state in Fig. 2 where the broken curve is drawn through the data points only to guide the eye). The agreement between the angular distributions of the strongly excited states and the DWBA calculations is general-

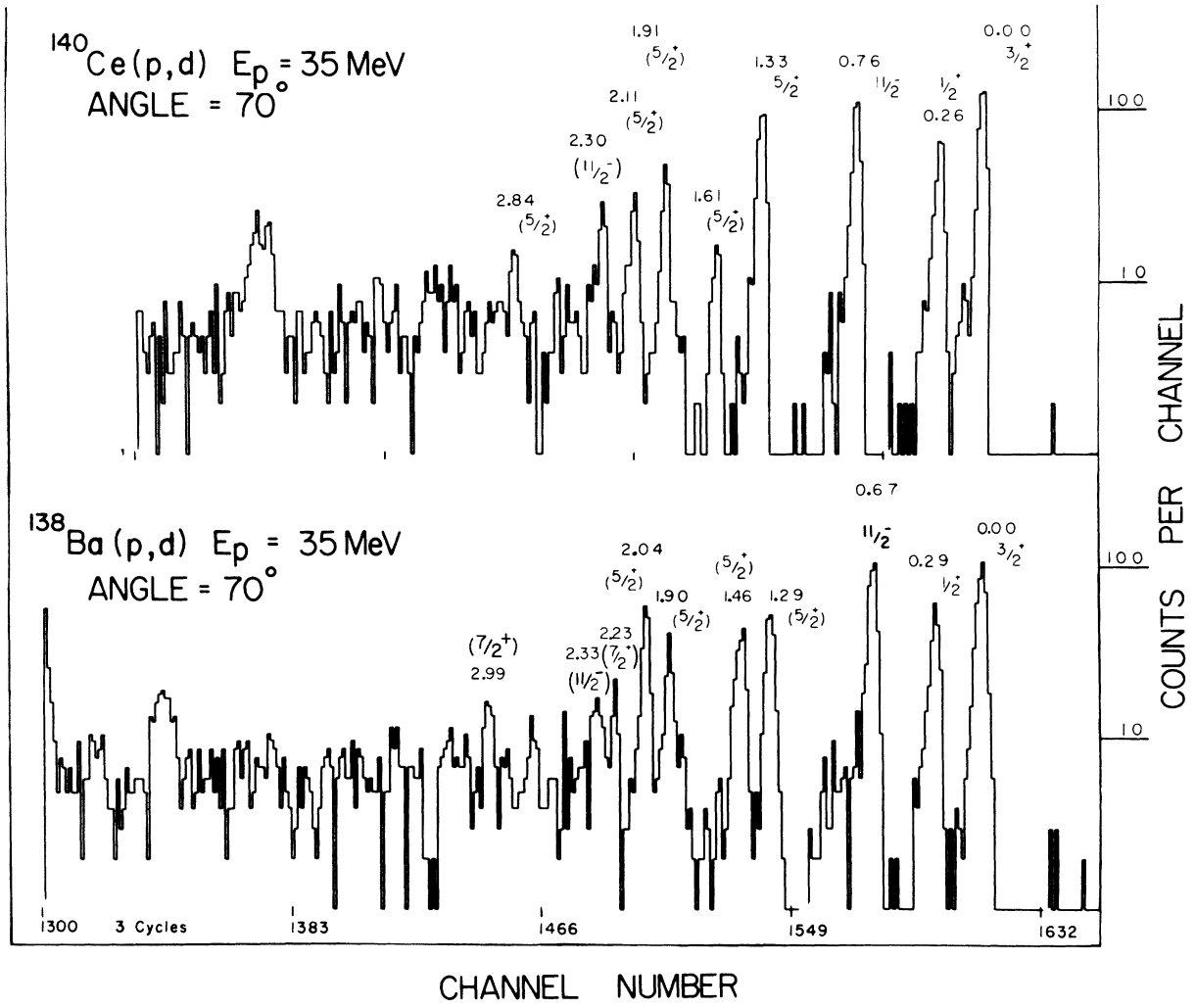

FIG. 1. Sample spectra from (p, d) reactions on ^{140}Ce and ^{138}Ba.

ly good with the exception of the 0.26-MeV ($l=0$, Fig. 2) state where only the locations of the maxima and minima and the general trend of the angular distribution are approximately reproduced.

In Fig. 3, six $l=2$ angular distributions are presented. The excitation energies of the states in ^{139}Ce that these correspond to are given on the right-hand side of each angular distribution. The ground state of ^{139}Ce is known[10] to be $\frac{3}{2}^+$ and its angular distribution agrees reasonably well with the DWBA calculation for $l=2$, $j=\frac{3}{2}$. The first excited state with an $l=2$ angular distribution is observed at an excitation energy of 1.33 MeV. This state is as strongly excited as the ground state and is assigned $J=\frac{3}{2}$ on the basis of sum-rule arguments given below. In the lower part of Fig. 6, the practically identical angular distributions for the ground states of ^{139}Ce and ^{137}Ba have been combined and compared with the similarly combined angular distributions for the first $l=2$, $j=\frac{5}{2}$ excited states in both of these nuclei to reveal any j-dependent effects. As in the case of ^{143}Sm and ^{141}Nd (top part of Fig. 6), the j-dependent effects are too weak (if any) to help one identify the j-value from the shape of the angular distribution.

Three states at 2.57, 2.84, and 3.20 MeV of excitation energy in the residual nucleus are observed to have angular distributions (Fig. 4) that can be candidates for an $l=4$ transfer. These angular distributions (with the exception of the angular distribution of the 3.20-MeV state), however, do not yield unambiguous l assignments.

In Fig. 5, two states at 0.76 and 2.30 MeV of excitation energy are observed to have $l=5$ angular distributions. The agreement of the angular distribution for the 0.76-MeV state with DWBA calculation is indeed good. The large error bars for the 2.30-MeV state data make its l assignment somewhat doubtful.

In Table III we give the excitation energies of the various states of ^{139}Ce observed here, along with their spins and parities (if assigned), differential cross sections at some suitably chosen angle, and absolute spectroscopic factors derived by use of Eq. (1) together with relative spectroscopic factors (based on the assumption that the spectroscopic factor for the $d_{3/2}$ ground state is 4.0; see below for a listing of reasons for this assumption). The

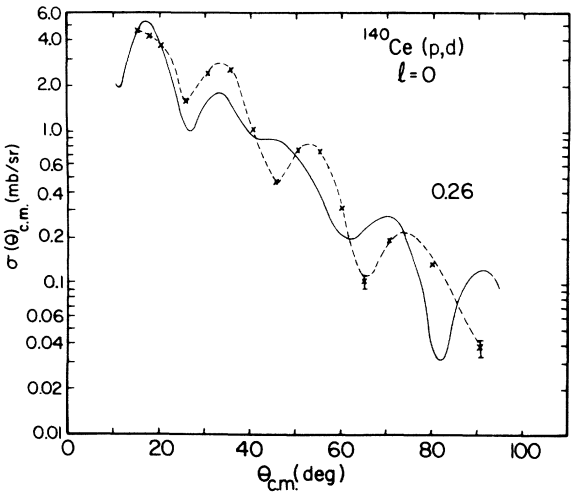

FIG. 2. A comparison of the experimental angular distribution for the 0.26-MeV state in ^{139}Ce$(d,p)^{140}$Ce with the FRNL DWBA calculation for $l=0$. The broken curve is drawn through the data points only to guide the eye.

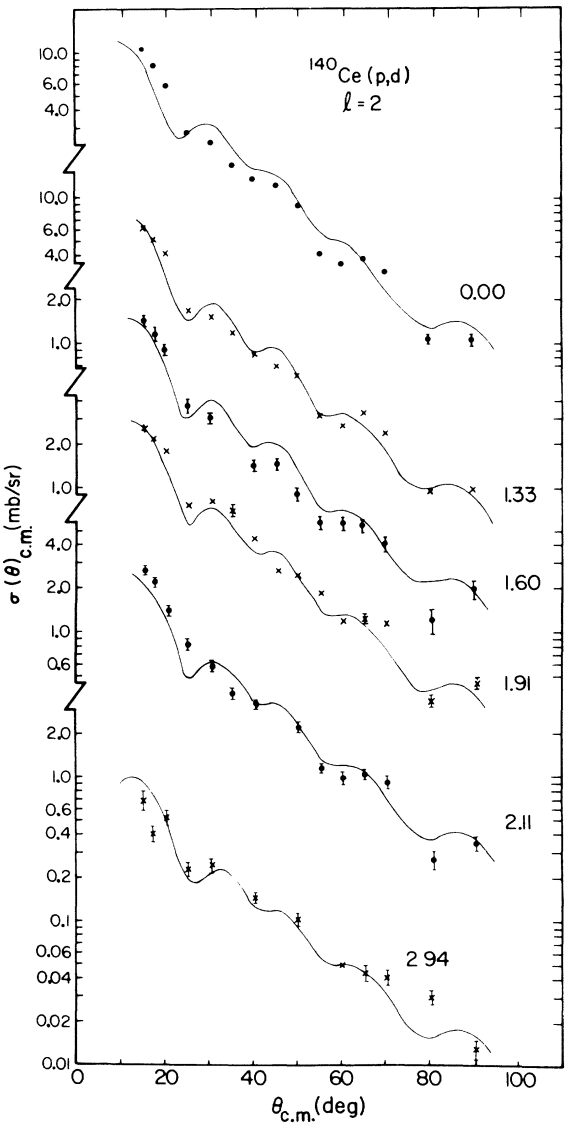

FIG. 3. A comparison of the experimental and FRNL DWBA angular distributions for $l=2$ in ^{140}Ce$(p,d)^{139}$Ce. Only the ground state of ^{139}Ce is assumed to have $J^\pi=\frac{3}{2}^+$. The excitation energies of the various states are shown on the right-hand side.

only ambiguity in J^π assignment occurs in the case of high-lying $l=2$ transitions. However, one can make the following plausibility arguments in favor of a $J^\pi=\frac{5}{2}^+$ assignment to the higher-lying $l=2$ states:

(i) As we shall see in Sec. IV (Fig. 13), in all cases studied in the (p, d) reactions on $N=82$ nuclei in the present sequence there is an energy gap $\gtrsim 1$ MeV between the ground state and the first excited $l=2$ state.

(ii) The ground state exhausts practically all of the $(d_{3/2})_\nu^{-1}$ strength. Assuming all the $l=2$ states at higher excitation energies to be $\frac{5}{2}^+$ yields consistent values of the total $(d_{5/2})_\nu^{-1}$ strength and centroid energies in all $N=81$ nuclei investigated in this paper and Paper I (see Fig. 14).

(iii) The shell-model ordering of the $d_{3/2}$ and the $d_{5/2}$ states observed in the present work [i.e., the $(d_{5/2})_\nu^{-1}$ state lies deeper in $N=82$ nuclei] is consistent with the $(d, {}^3\mathrm{He})$ and (t, α) studies made on the $Z=82$ Pb nuclei.[11]

(iv) Assuming that all the high-lying $l=2$ states are of spin and parity $\frac{5}{2}^+$, it is apparent that the $(d_{5/2})_\nu^{-1}$ state has split into at least five components. An energy systematics of these components in all $N=81$ nuclei studied here is given in Fig. 13 of Sec. IV. Assigning $J^\pi=\frac{3}{2}^+$ even to one of the weaker $l=2$ transitions in $^{144}\mathrm{Sm}(p, d)^{143}\mathrm{Sm}$ would mean too large a strength for the $(d_{3/2})_\nu^{-1}$ state and too small a strength for the $(d_{5/2})_\nu^{-1}$ state in $^{137}\mathrm{Ba}$. On the basis of these arguments, tentative spin and parity assignments of $\frac{5}{2}^+$ have been made to all the high-lying $l=2$ states in all $N=81$ nuclei studied here.

The energy levels of $^{139}\mathrm{Ce}$ along with their J^π as-

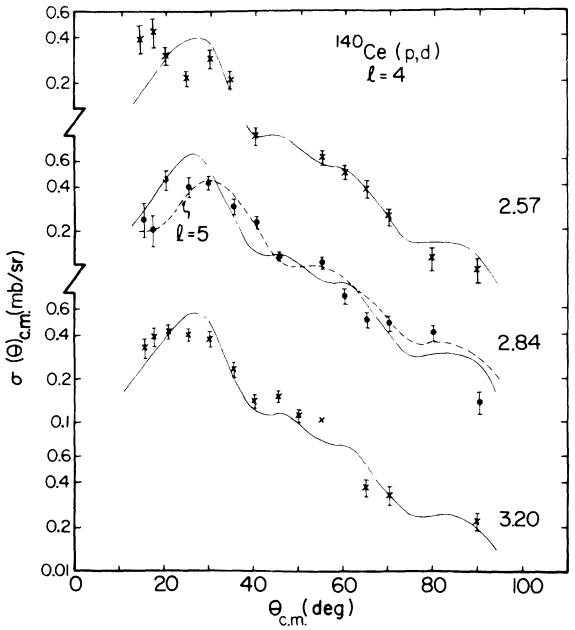

FIG. 4. A comparison of the experimental and FRNL DWBA angular distributions for $l=4$ in $^{140}\mathrm{Ce}(p, d)^{139}\mathrm{Ce}$. The data for the 2.84-MeV state have also been compared with a DWBA calculation of $l=5$ (broken curve).

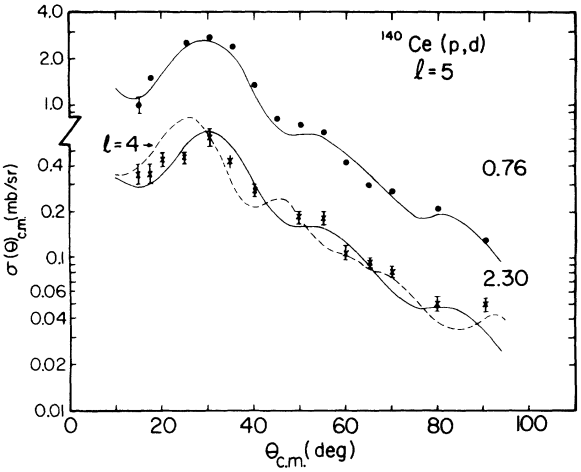

FIG. 5. A comparison of the experimental and FRNL DWBA angular distributions for $l=5$ in $^{140}\mathrm{Ce}(p, d)^{139}\mathrm{Ce}$. The data for the 2.30-MeV state have also been compared with a DWBA calculation for $l=4$.

The energy levels of $^{139}\mathrm{Ce}$ along with their J^π as-

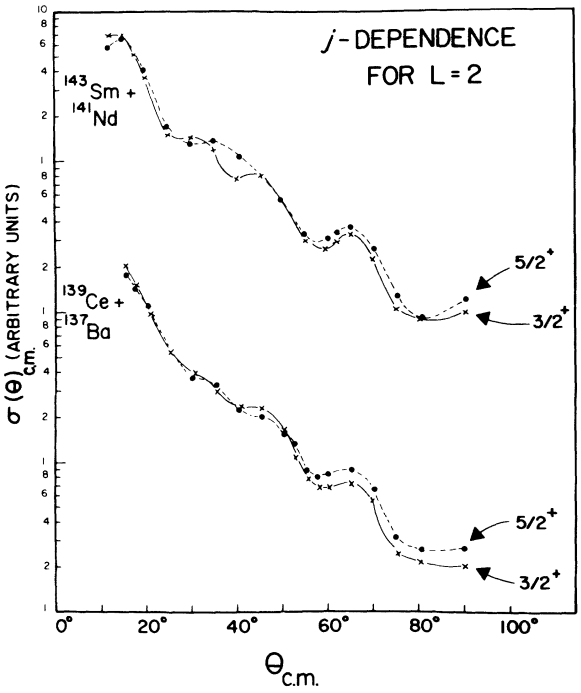

FIG. 6. Comparison of the $d_{3/2}$ ground state and the first excited (and also the strongest) $d_{5/2}$ state angular distributions to indicate any possible j-dependent effects. The $d_{3/2}$ $(d_{5/2})$ angular distributions for both $^{139}\mathrm{Ce}$ and $^{137}\mathrm{Ba}$ are very similar and were, therefore, combined to average out fluctuations that might mask any systematic j-dependent effects. The data for $^{143}\mathrm{Sm}$ and $^{141}\mathrm{Nd}$ are taken from Ref. 1.

signments and spectroscopic factors are shown in Fig. 7, where these have been compared with the results of Yagi *et al.*[12]; Fulmer, McCarthy, and Cohen[13]; and the unpublished results of Bruge *et al.*[14] Our spin and parity assignments are largely in agreement with those of other experiments, the exceptions being the 2.30- and the 2.94-MeV states. In the former case our angular distribution (well predicted by FRNL DWBA calculations for the other $\frac{11}{2}^-$ state) seems to agree better (Fig. 5) with the DWBA calculation for $l=5$ indicating it to be an $\frac{11}{2}^-$ state. This is further supported by the energy systematics of the two components of the $(1h_{11/2})_\nu^{-1}$ state observed in all $N=81$ nuclei in the present work and discussed in Sec. IV (see Fig. 13). The difference between the shapes for $l=4$ and $l=5$ DWBA calculations is not very large; hence the uncertainty in these large l-value assignments for some weakly excited states. The situation is somewhat uncertain in the case of the 2.94-MeV state because of the high density of states in this region of excitation energy. Our angular distribution agrees well with the DWBA calculation for $l=2$; hence the spin and parity assignment of $\frac{5}{2}^+$.

The 1.79-MeV state was first noticed in the high-resolution position-sensitive detector measurements and was later sought in the counter telescope spectra. Its intensity in the latter spectra is only 5–10% of the intensity of the 1.91-MeV state, so that an angular distribution could not be obtained as this group is resolved from the tail of the neighboring 1.91-MeV state at only a few angles. Consequently, even the existence of this state is somewhat in doubt. It was tentatively assigned a spin and parity of $\frac{1}{2}^+$ only on the basis of the energy systematics of the second $\frac{1}{2}^+$ state in the level spectra of all the $N=81$ nuclei studied in Paper I and here (see Fig. 13).

TABLE III. Excitation energies, l and J^π assignments, (p, d) cross sections at the observation angle θ, and absolute and relative spectroscopic factors for the various states observed in the ^{140}Ce$(p, d)^{141}$Ce reaction.

Excitation energy (MeV)	l	J^π	$\theta_{c.m.}$ (deg)	$\sigma(\theta)_{c.m.}$ (mb/sr)	S	S (relative)
0.00	2	$\frac{3}{2}^+$	25.3	2.80	4.6	4.0
0.26	0	$\frac{1}{2}^+$	20.2	3.65	1.6	1.4
0.76	5	$\frac{11}{2}^-$	25.3	2.50	8.1	7.0
1.33	2	$(\frac{5}{2}^+)$	25.3	1.70	3.0	2.6
1.60	2	$(\frac{5}{2}^+)$	25.3	0.37	0.7	0.6
(1.79)	(0)	$(\frac{1}{2}^+)$	20.2	0.15	0.08	0.07
1.91	2	$(\frac{5}{2}^+)$	35.4	0.70	1.2	1.1
2.11{2.10, 2.14}	2	$(\frac{5}{2}^+)$	40.4	0.31	1.1	0.9
2.30	(5)	$(\frac{11}{2}^-)$	20.2	0.44	2.0	1.8
(2.37)	...	...	20.2	0.1	...	...
(2.47)	...	...	20.2	0.1	...	...
2.57	(4)	$(\frac{7}{2}^+)$	40.4	0.088	2.0	1.8
2.84	(4)	$(\frac{7}{2}^+)$	45.5	0.137	3.2	2.7
2.94	(2)	$(\frac{5}{2}^+)$	25.3	0.23	0.5	0.4
3.20	(4)	$(\frac{7}{2}^+)$	20.2	0.41	3.0	2.6
3.37	...	...	20.2	0.69	...	...

The relative spectroscopic factors obtained in the present work have also been compared with those obtained by Yagi *et al.*[12] Their spectroscopic factors for the low-lying and strongly excited (see Fig. 1) $\frac{1}{2}^+$ and $\frac{11}{2}^-$ states are ~30% higher than our values even though the two sets of spectroscopic factors agree for the $(2d_{3/2})_\nu^{-1}$ and the $(2d_{5/2})_\nu^{-1}$ states. This apparently indicates an l (or orbital Nlj) dependent effect in the DWBA calculations. The DWBA calculations of Yagi *et al.*[12] are of the zero-range variety and use a code[15] different from the one used in the present work. Our study of the effects of including FRNL corrections in the DWBA calculations (see Paper I) indicates that the spectroscopic factors for $l=4$ transitions should decrease and those for $l=5$ should increase relative to the spectroscopic factors for $l=2$ transitions. But the comparison between the spectroscopic factors of Yagi *et al.*[12] and the present work shows trends contrary to these expectations, leading one to speculate that barring any errors, the 55-MeV data of Yagi *et al.*[12] may be showing a sensitivity to the details of the form factor in the nuclear interior greater than our 35-MeV measurements do. If this is correct, energy dependence of these spectroscopic factors may prove very valuable in learning the details of the form factor in these transitions.

Values of the single-neutron-hole energies [derived by using Eq. (3)] for the various filled shell-model orbits in the $50<N\leq 82$ region were calculated relative to $E_{d_{3/2}}$ and are listed in Table IV along with the summed hole strengths for these states. The summed strengths are given in absolute and relative values (obtained by assuming $S_{d_{3/2}}=4.0$) and have been compared with theoretical values [calculated from Eq. (2)] and those of Yagi *et al.*[12] The proton occupation probabilities for calculating the theoretical spectroscopic factors were taken from the $(d, {}^3\mathrm{He})$ and $({}^3\mathrm{He}, d)$ studies of Wildenthal, Newman, and Auble.[16] It is apparent from an examination of Table IV that ~30% of the strength for both the $(3s_{1/2})_\nu^{-1}$ and the $(1h_{11/2})_\nu^{-1}$ states is missing. An examination of Fig. 14 of Sec. IV will reveal that we are missing some $(1h_{11/2})_\nu^{-1}$ strength in all $N=81$ nuclei studied in the

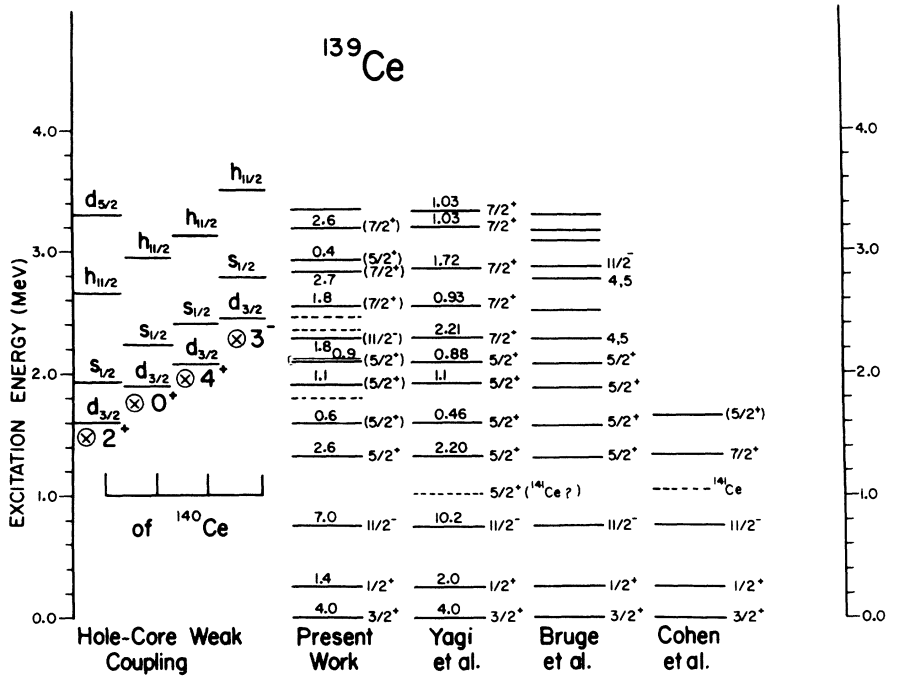

FIG. 7. A comparison of the present results in ^{140}Ce$(p,d)^{139}$Ce with the results of Yagi *et al.* (Ref. 12), the preliminary results of Bruge *et al.* (Ref. 14), and the results of Fulmer, McCarthy, and Cohen (Ref. 13). The numbers above the energy levels in the present work and that of Yagi *et al.* are relative spectroscopic factors. A comparison is also made between the neutron-hole states weakly coupled to the 2^+, 0^+, 4^+, and the 3^- core excitations of ^{140}Ce and the ^{139}Ce energy levels. See text for further comments.

present sequence (see further discussion in Sec. IV). In the case of the $(3s_{1/2})_\nu^{-1}$ state, the loss of strength is probably due to the fact that we were unable to definitely identify any excited $l=0$ states. The $l=0$ assignment to the 1.79-MeV state is purely on the basis of energy systematics (Fig. 13). However, this state does not have enough cross section to account for the missing $(3s_{1/2})_\nu^{-1}$ strength.

The centroid energies of Yagi *et al.*[12] have also been compared with those from the present work. The lower energies of Yagi *et al.*[12] for $(1h_{11/2})_\nu^{-1}$ and $(3s_{1/2})_\nu^{-1}$ states merely reflect the fact that they see only the strongest of the two components (see Fig. 7) of these states. The differences in the other two centroid energies are probably due to uncertainties in the determination of the relative

TABLE IV. Sums of spectroscopic strengths and centroids of single-neutron-hole energies (MeV).

	Absolute	$(\sum_i S_i)_{Nlj}$ Relative		Theor.	$\bar{E}_{Nlj}-\bar{E}_{2d_{3/2}}=\frac{(\sum_i S_i E_i)_{Nlj}}{(\sum_i S_i)_{Nlj}}$	
Nlj		(Present work)	(Ref. 13)		(Present work)	(Ref. 13)
			^{139}Ce			
$2d_{3/2}$	4.6	4.0	4.0	4.0	0.00	0.00
$3s_{1/2}$	1.6	1.45	2.0	2.0	0.33	0.25
$1h_{11/2}$	10.1	8.7	10.2	12.0	1.07	0.75
$2d_{5/2}$	6.5	5.6	5.0	6.0	1.72	1.60
$1g_{7/2}$	8.2	7.1	7.4	7.9	2.90	2.81
			^{137}Ba			
$2d_{3/2}$	3.4	4.0		4.0	0.00	
$3s_{1/2}$	1.53	1.80		2.0	0.54	
$1h_{11/2}$	7.8	8.4		12.0	1.07	
$2d_{5/2}$	5.1	6.1		6.0	1.71	
$1g_{7/2}$	7.3	8.6		7.9	2.93	

spectroscopic factors.

In Fig. 7, the energy levels of ^{139}Ce have also been compared with the centers of gravity of states derived from the weak coupling of the neutron-hole states and the core-excited 2^+, 0^+, 4^+, and the 3^- states of ^{140}Ce. The agreement between the energies of the $(2d_{3/2})_\nu^{-1}\otimes 2^+$ state and the 1.60-MeV $\frac{5}{2}^+$ state seems to suggest that perhaps the 1.60-MeV state has an appreciable component of $(2d_{3/2})_\nu^{-1}\otimes 2^+$ in its wave function. Similar comments could also be made about the 1.91- and 2.10-MeV states.

B. ^{138}Ba$(p, d)^{137}$Ba

A deuteron energy spectrum from this reaction measured at 70° is shown in the bottom part of Fig. 1. As in ^{140}Ce(p, d), the lowest three prominent peaks represent the dominant components of $(2d_{3/2})_\nu^{-1}$, $(3s_{1/2})_\nu^{-1}$, $(1h_{11/2})_\nu^{-1}$ states in the $N=82$ core. Angular distributions of these and several other deuteron groups seen in Fig. 1 have been measured from 15 to 90° and compared with FRNL DWBA calculations. The results of these comparisons are shown in Figs. 8–11.

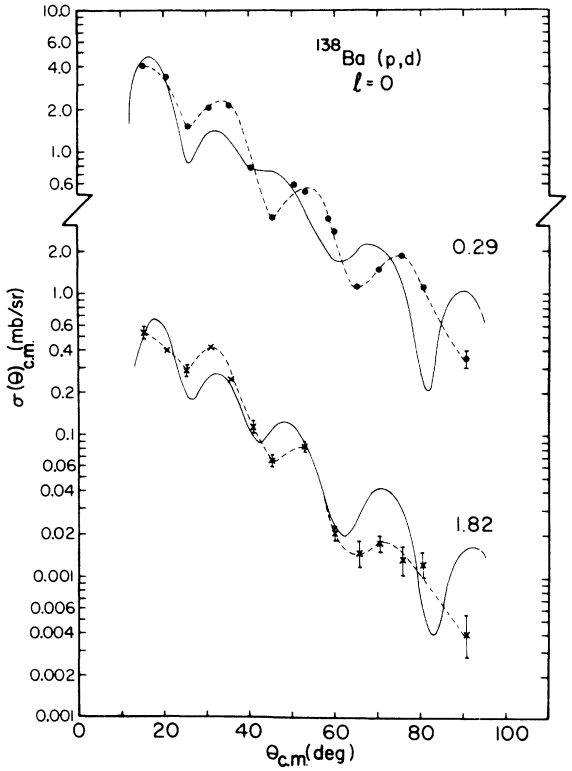

FIG. 8. A comparison of the experimental and FRNL DWBA angular distributions for $l=0$ in ^{138}Ba$(p,d)^{137}$Ba. The broken curves drawn through the experimental points are merely to guide the eye.

Two $l=0$ groups at excitation energies of 0.29 and 1.82 MeV can be seen in Fig. 8. The broken curves going through the data points merely guide the eye. The DWBA cross sections for $l=0$ only qualitatively agree with the experimental angular distributions.

Next, in Fig. 9 are shown five $l=2$ angular distributions, the shapes of which are reproduced reasonably well by the FRNL DWBA calculations. For reasons given in the section on ^{140}Ce$(p, d)^{139}$Ce only the ground state was assumed to have a spin parity of $\frac{3}{2}^+$; all others were assigned $J^\pi=\frac{5}{2}^+$. An examination of the energy systematics of these $l=2$ (see Fig. 13 in Sec. IV) reveals that such a choice of spin and parity for the higher $l=2$ states

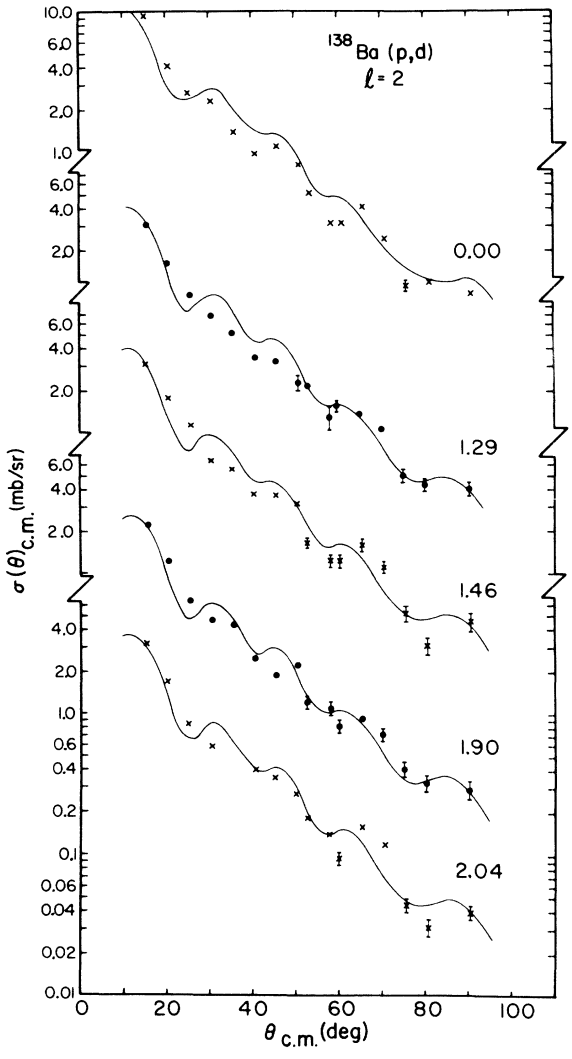

FIG. 9. A comparison of the experimental and FRNL DWBA angular distributions for $l=2$ in ^{138}Ba$(p,d)^{137}$Ba. Only the ground state of ^{137}Ba is assumed to have a $J^\pi=\frac{3}{2}^+$. The numbers on the right-hand side are excitation energies in MeV.

is inconsistent with a similar choice in other $N = 81$ nuclei.

In Fig. 10 four $l = 4$ angular distributions corresponding to 2.23, 2.54, 2.99, and 3.55 MeV of excitation energy in the residual nucleus can be seen. The experimental angular distributions agree well with the FRNL DWBA calculations for $l = 4$. Both $l = 4$ and 5 calculations have been compared with the data for the 2.54-MeV state to show the difference (or similarity) in the degree of agreement of the two calculations with the experimental angular distribution.

Two angular distributions are shown in Fig. 11 for groups corresponding to excitation energies of 0.67 and 2.33 MeV in ^{137}Ba. Both $l = 4$ and $l = 5$ DWBA calculations have been compared with the angular distribution for the 2.33-MeV group. The data seem to agree better with the $l = 5$ angular distribution. The energy of this group is consistent with the energy systematics of the second component of the $(1h_{11/2})_v^{-1}$ state (Fig. 13) thus confirming our tentative $l = 5$ assignment.

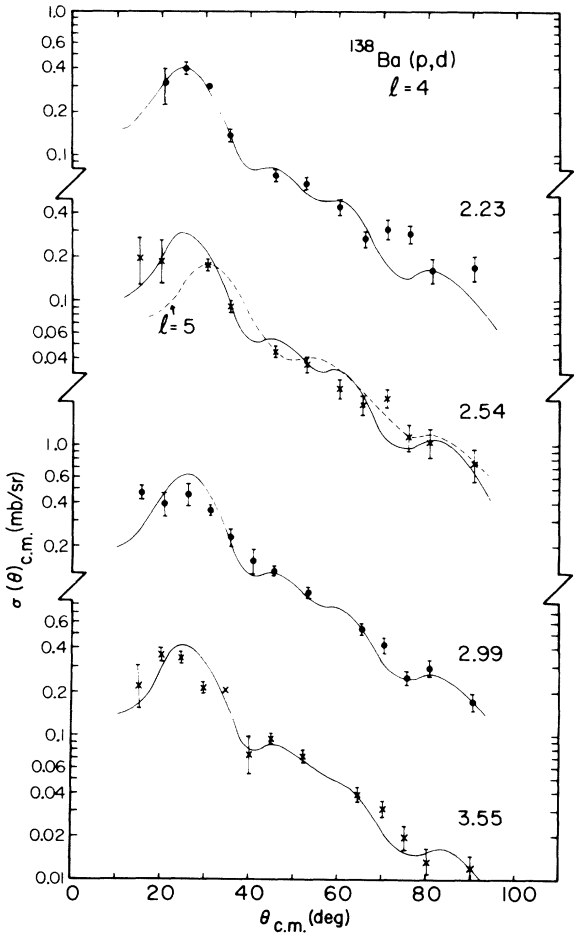

FIG. 10. A comparison of the experimental and FRNL DWBA angular distributions for $l = 4$ in ^{138}Ba$(p, d)^{137}$Ba. The data for the 2.54-MeV state have also been compared with a DWBA calculation for $l = 5$ (broken curve).

The excitation energies of the various states observed in ^{138}Ba$(p, d)^{137}$Ba along with their spins and parities, differential cross sections at some suitably chosen angles, absolute spectroscopic factors obtained by using (1) together with relative spectroscopic factors (i.e., when $S_{d_{3/2}} = 4.0$) are listed in Table V. The uncertainty in the $\frac{5}{2}^+$ assignment for all the excited $l = 2$ states is due to the fact that these assignments were not based on any j-dependent effects. No meaningful angular distributions could be obtained for the 2.74 and the 2.90-MeV states. The states within parentheses were observed in at least three different spectra at different angles but no angular distribution could be measured. Hence it is concluded that their existence needs further confirmation.

Figure 12 shows the energy levels of ^{137}Ba along with their spins, parities, and relative spectroscopic factors. These have been compared with the unpublished (p, d) results of Bruge *et al.*,[14] the (d, t) measurements of Cohen *et al.*[13] and the (d, p)

TABLE V. Excitation energies, l and J^π assignments, (p, d) cross sections at the observation angle θ, absolute and relative spectroscopic factors for the various states observed in the ^{138}Ba$(p, d)^{137}$Ba reactions.

Excitation energy (MeV)	l	J^π	$\theta_{c.m.}$ (deg)	$\sigma(\theta)_{c.m.}$ (mb/sr)	S	S (relative)
0.00	2	$\frac{3}{2}^+$	50.6	0.78	3.4	4.0
0.29	0	$\frac{1}{2}^+$	20.2	3.4	1.3	1.5
0.67	5	$\frac{11}{2}^-$	25.3	2.5	6.4	7.6
1.29	2	$(\frac{5}{2}^+)$	25.3	0.98	1.3	1.6
1.46	2	$(\frac{5}{2}^+)$	25.3	1.18	1.5	1.7
1.82	0	$\frac{1}{2}^+$	40.4	0.112	0.25	0.29
1.90	2	$(\frac{5}{2}^+)$	25.3	0.66	1.0	1.2
2.04	2	$(\frac{5}{2}^+)$	25.3	0.84	1.3	1.5
2.23	4	$\frac{7}{2}^+$	25.3	0.40	1.5	1.8
2.33	5	$\frac{11}{2}^-$	45.5	0.14	1.4	1.7
2.54	4	$\frac{7}{2}^+$	35.4	0.093	1.0	1.2
2.74	...	...	59.6	0.04	...	...
2.90	...	...	59.6	0.03	...	...
2.99	4	$\frac{7}{2}^+$	35.4	0.23	2.7	3.2
(3.13)	...	...	59.6	0.04	...	...
(3.21)	...	...	59.6	0.06	...	...
(3.42)	...	...	59.6	0.03	...	...
3.55	4	$\frac{7}{2}^+$	20.2	0.36	2.0	2.4

measurements of Von Ehrenstein *et al.*[17] With the exception of the 2.99-MeV state our spin and parity assignments agree quite well with those from the other two neutron pickup experiments. Bruge *et al.*[14] claim this state to be of spin and parity $\frac{11}{2}^-$. Our angular distribution (Fig. 10) agrees very well with the $l=4$ DWBA calculation and will not agree with the calculation for $l=5$. The energy systematics of the various $l=4$ and $l=5$ states (Fig. 13) also support our J^π assignment of $\frac{7}{2}^+$.

A significant point in the comparison with the ^{136}Ba$(d,p)^{137}$Ba measurement of Von Ehrenstein *et al.*[17] is that we do not see any $\frac{7}{2}^-$, $\frac{3}{2}^-$, or $\frac{1}{2}^-$ states with any measurable intensity ($\gtrsim$0.05 mb/sr). If 82 neutrons do not form a good closed shell, then the lowest orbital to have a nonzero occupation probability would be $(2f_{7/2})_\nu^{-1}$ as we know from the (d,p) studies on $N=82$ nuclei.[17,18] The occupation probability of the higher neutron single-particle orbits will be certainly less than that of the $2f_{7/2}$ orbit. Since no measurable cross section for pickup from the $2f_{7/2}$ orbit has been observed here (or in any other $N=81$ nucleus studied in the present program[1]) at excitation energies expected for these states, it must be assumed that the shell closure at $N=82$ is reasonably good.

The "centers of gravity" of the various neutron-hole-state components along with their summed hole strengths are listed in Table IV. The summed strengths are given in relative (i.e., $S_{d_{3/2}}=4.0$) and absolute values and have been compared with theoretical values derived from Eq. (2) where the proton occupation numbers for the shell-model orbits of interest were obtained from the (^{3}He, d) and (d, ^{3}He) measurements of Wildenthal, Newman, and Auble.[16] With the exception of the $(1h_{11/2})_\nu^{-1}$ state the relative and absolute strengths are in good agreement (within the uncertainties of the present measurements) with the theoretical estimates. The strength of the $(1h_{11/2})_\nu^{-1}$ state seems to have been underestimated as has been found to be the case with other $N=81$ nuclei (see discussion in Sec. IV).

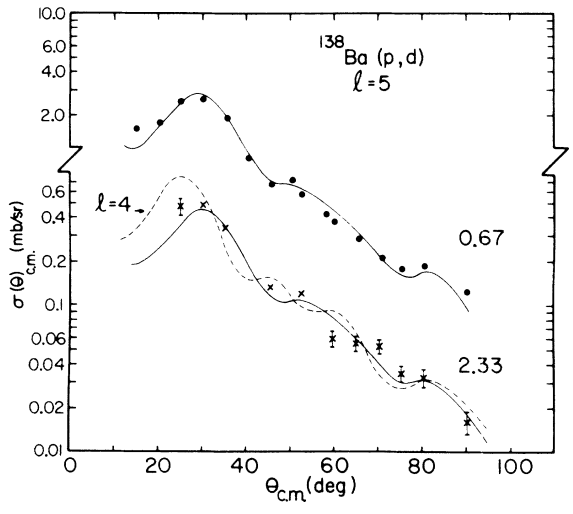

FIG. 11. A comparison of the experimental and FRNL DWBA angular distributions for $l=5$ in ^{138}Ba$(p,d)^{137}$Ba. The data for the 2.33-MeV state have also been compared with a calculation for $l=4$ (broken curve).

The neutron-single-hole energies listed are very similar to those obtained in the case of ^{139}Ce (the exception being the $3s_{1/2}$ state). A detailed discussion of the centroid energies and their movement with Z is presented in the following section.

IV. HOLE STATES IN $N=81$ NUCLEI

A. Fractionation and Hole-Core Coupling

Figure 13 presents the combined results of Paper I and the present paper on the excitation energies and the relative spectroscopic factors of the components of the various neutron-hole states in the $N=81$ nuclei investigated here. The data have been grouped according to orbital angular momentum of the transferred nucleon in the (p,d) reactions on ^{144}Sm, ^{142}Nd, ^{140}Ce, and ^{138}Ba, and are discussed below in order of increasing angular momentum.

(i) $(3s_{1/2})_\nu^{-1}$ *(L=0).* Two components are observed for the $(3s_{1/2})_\nu^{-1}$ state in three of the four nuclei. We saw a state at the energy of the broken line in ^{139}Ce. No angular distribution could be measured, so that the existence of this second $l=0$ state in ^{139}Ce is somewhat doubtful. Most of the strength is found in the lower component in all four nuclei.

(ii) $(2d_{5/2})_\nu^{-1}$ *(L=2).* As discussed in Sec. III, the ground states have been assumed to be $\frac{3}{2}^+$ containing all of the strength of the $(2d_{3/2})_\nu^{-1}$ state. On this basis, five components of the $(2d_{5/2})_\nu^{-1}$ state are observed in all $N=81$ nuclei studied here except ^{137}Ba. Four of these five components lie between 1.1 and 2.1 MeV of excitation energy. In ^{143}Sm the lowest of these four components contains the lion's share of the $(2d_{5/2})_\nu^{-1}$ strength. As one observes the systematics of these components from ^{143}Sm to ^{137}Ba, one notices that (1) the strength gets more evenly distributed between the four components, and (2) the energy spread of the components decreases. Another noticeable feature of this systematics is the presence of a $(2d_{5/2})_\nu^{-1}$ component at ~3.0 MeV of excitation energy. This latter component was sought for and not found in ^{137}Ba.

(iii) $(1g_{7/2})_\nu^{-1}$ *(L=4).* The situation for the components of this neutron-hole state is far less certain than is the case with other neutron-hole states, because of the smaller cross sections for these

states. In general four components are observed with comparable strengths. The most notable feature of the systematics of these components is the fact that states with ~$\frac{1}{3}$ of the total strength are observed at 1.4 MeV of excitation energy in ^{143}Sm and ^{141}Nd but no analogous states are observed in ^{139}Ce or ^{137}Ba. There are strongly excited $d(l=2)$ states at excitation energies where these $g_{7/2}$ states may be expected to occur in ^{139}Ce and ^{137}Ba. A reexamination of the energy spectra and the angular distributions for these d states in ^{139}Ce and ^{137}Ba did not reveal any evidence for unresolved doublets. On the other hand, a comparison of the summed $(1g_{7/2})_v^{-1}$ strengths in all $N=81$ (e.g., see Fig. 14) shows that some strength is lost in ^{139}Ce and ^{137}Ba as compared to ^{143}Sm and ^{141}Nd despite the large uncertainties (~15%) in $(1g_{7/2})_v^{-1}$ cross sections. Repeat measurements with higher resolution ($\Delta E < 10$ keV) and a low background might enable one to locate the missing $(1g_{7/2})_v^{-1}$ strength.

(iv) $(1h_{11/2})_v^{-1}$ *(L = 5).* At least two components are observed in all nuclei with most of the $(1h_{11/2})_v^{-1}$ strength being in the lower component. In ^{143}Sm a third component is observed very close to the second. The l assignment for this third component is not as certain as it is for the other two components (Paper I).

In Table VI we list the possible origins of the various components of the single-neutron-hole states by assuming that these neutron-hole states, in addition to being coupled to the ground state of the target nucleus, may also couple to some strongly excited states of the core (e.g., the first excited 2^+ and the collective 3^- states), giving rise to states of the same J^π as the neutron-hole states. The two types of states of the same J^π can then mix thus giving each mixed state an excited core component in its total wave function. For example consider the $(2d_{5/2})_v^{-1}$ state with $J^\pi = \frac{5}{2}^+$. Another state of $J^\pi = \frac{5}{2}^+$ may be built from coupling the $(2d_{3/2})_v^{-1}$ to the first excited 2^+ state. Both of these states can mix giving rise to two other states,

$$\psi_1^{5/2^+} = a[(2d_{5/2})_v^{-1} \otimes 0^+_{\text{g.s.}}]_{5/2^+} + b[(2d_{3/2})_v^{-1} \otimes 2^+]_{5/2^+}$$

and

$$\psi_2^{5/2^+} = -b[(2d_{5/2})_v^{-1} \otimes 0^+_{\text{g.s.}}]_{5/2^+} + a[(2d_{3/2})_v^{-1} \otimes 2^+]_{5/2^+},$$

where ψ_1 and ψ_2 are orthogonal. The cross section for observing ψ_1 in a (p, d) reaction depends on $|a|^2$. If a is small, the (p, d) cross section may be practically unmeasurable. This might explain why more possible components are listed in Table VI than are observed in the present (p, d) measurements.

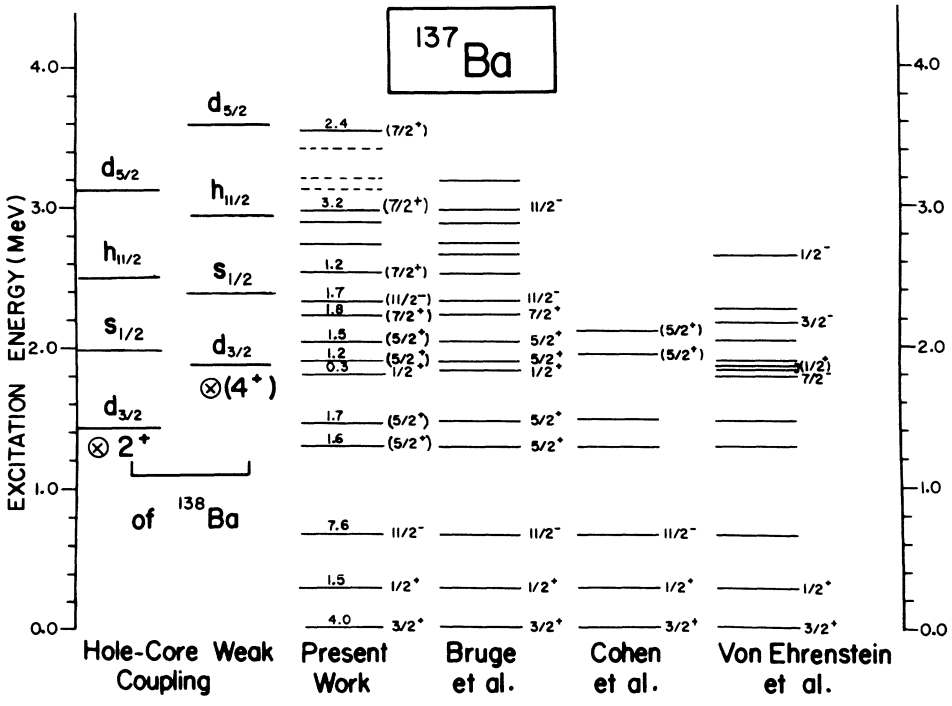

FIG. 12. A comparison of the present results in ^{138}Ba(p,d) with the unpublished results of Bruge *et al.* (Ref. 14), those of Fulmer, McCarthy, and Cohen (Ref. 13), and Von Ehrenstein *et al.* (Ref. 17). The numbers above the energy levels in the present work are relative spectroscopic factors. A comparison is also made between the neutron-hole states weakly coupled to the 2^+ and the 3^- core excitation of ^{138}Ba with the ^{137}Ba energy levels. See text for further comments.

by using a central and a tensor component for the effective *pn* interaction. In the nuclei considered here (Fig. 14), the $1g_{9/2}$ proton orbit is assumed completely filled while the occupation of the $1g_{7/2}$ changes slightly as a function of Z, so that the total population of the g protons is practically constant in going through these nuclei. The $2d_{5/2}$ proton orbit, however, is filling more rapidly so that following the work of Yagi, one would expect the binding energy of the d (both $\frac{3}{2}^+$ and $\frac{5}{2}^+$) and the $s_{1/2}$ states to increase relative to that of the $1g_{7/2}$ state, or alternatively, their energy spacing relative to $1g_{7/2}$ decrease with increasing Z in these nuclei. Figure 14 bears out the expectations outlined above. The trend of the $(1h_{11/2})_\nu^{-1}$ state is also in agreement with the results of Yagi.

C. Sum Rule

The summed relative spectroscopic strengths (i.e., $S_{d_{3/2}} = 4.0$) for the various hole states are indicated above each state in Fig. 15. It is difficult to estimate the uncertainty in these numbers but ~20% (combining both the experimental and the DWBA uncertainties) is perhaps a reasonable guess. Most of the spectroscopic sums are in agreement with their theoretical values (2) for all

TABLE VI. Possible origin of components of single-neutron-hole states from the coupling of these hole states in the 2^+, 4^+, and 3^- excited states of the target ($N = 82$) nuclei. Coupling to excited 0^+ states will give rise to states of the same spin and parity as the neutron-hole states. See Sec. IV for further discussion.

	$\frac{3}{2}^+$	$\frac{1}{2}^+$	$\frac{11}{2}^-$	$\frac{5}{2}^+$	$\frac{7}{2}^+$
$2^+ \otimes \frac{3}{2}^+$	X	X		X	X
$2^+ \otimes \frac{1}{2}^+$	X			X	
$2^+ \otimes \frac{11}{2}^-$			X		
$2^+ \otimes \frac{5}{2}^+$	X	X		X	X
$2^+ \otimes \frac{7}{2}^+$	X			X	X
$4^+ \otimes \frac{3}{2}^+$				X	X
$4^+ \otimes \frac{1}{2}^+$					X
$4^+ \otimes \frac{11}{2}^-$			X		
$4^+ \otimes \frac{5}{2}^+$	X			X	X
$4^+ \otimes \frac{7}{2}^+$	X	X		X	X
$3^- \otimes \frac{3}{2}^+$					
$3^- \otimes \frac{1}{2}^+$					
$3^- \otimes \frac{11}{2}^-$				X	X
$3^- \otimes \frac{5}{2}^+$			X		
$3^- \otimes \frac{7}{2}^+$			X		

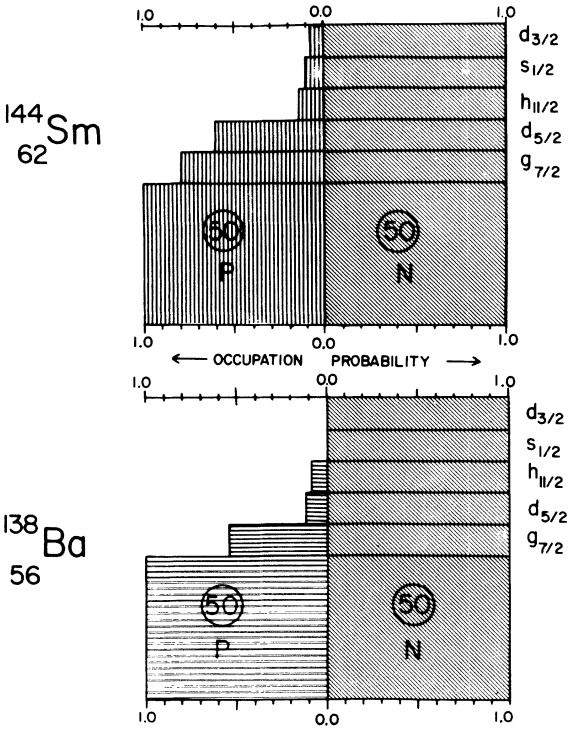

FIG. 14. Occupation probabilities of protons and neutrons in the $N = 82$ nuclei of ^{138}Ba and ^{144}Sm. The proton occupation probabilities were taken from the $(d, {}^3\text{He})$ and $({}^3\text{He}, d)$ measurements of Wildenthal, Newman, and Auble (Ref. 16).

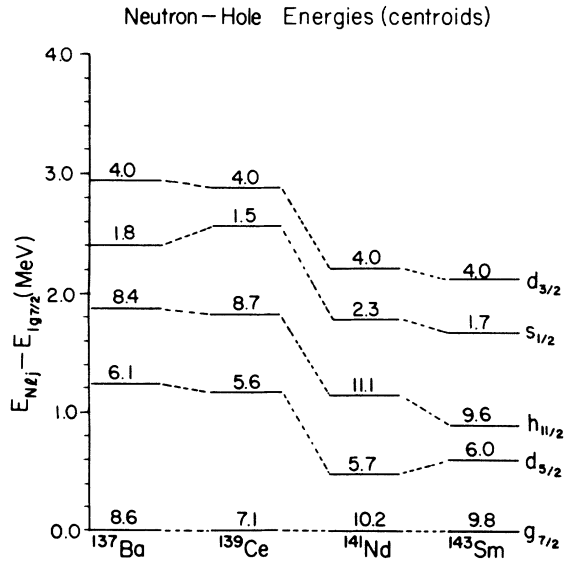

FIG. 15. Single-neutron-hole energies E_{Nlj}, measured relative to the energy of the $(1g_{7/2})_\nu^{-1}$ state. The numbers above the solid lines are summed relative spectroscopic strengths.

B. Neutron-Hole Energies

The centroid energies of the various neutron-hole states computed according to Eq. (3) have been plotted relative to the centroid energy of the $(1g_{7/2})_\nu^{-1}$ state to examine the trends in the variation of these energies as the valence protons increasingly fill some of the same shell-model orbits (i.e., $1g_{7/2}$, $2d_{5/2}$, $1h_{11/2}$, $3s_{1/2}$, and $2d_{3/2}$) as the neutrons in the $50 < N \leq 82$ range. The manner in which these proton orbits are being filled is shown in Fig. 14 where the proton occupation probabilities[16] for the lightest and the heaviest nuclei in the present set of $N = 82$ nuclei have been compared. It is apparent that the $1g_{7/2}$ and the $2d_{5/2}$ orbits are filling more rapidly as compared to the other three subshells. To describe the movement of the hole-state energies with increasing proton occupation, energy shift calculations involving the neutron-hole state and at least the valence protons (of Fig. 14) with some assumption about the effective *pn* interaction between them are necessary. Such calculations have been made by Yagi[2] which at least qualitatively describe the Z dependence of the neutron-hole energies in ^{91}Zr, ^{117}Sn, and ^{139}Ce

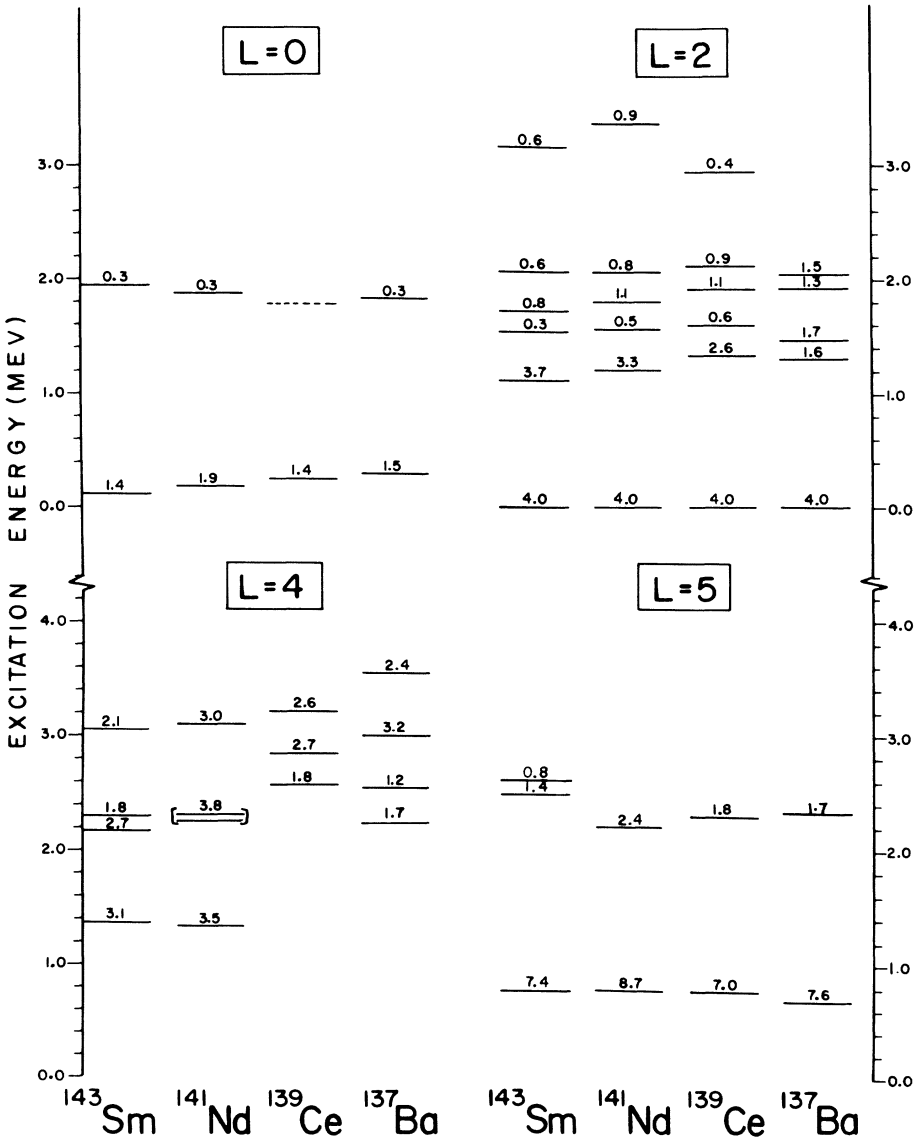

FIG. 13. Excitation energy and spectroscopic strength systematics of the various components of the $(3s_{1/2})_\nu^{-1}(L=0)$, $(2d_{3/2})_\nu^{-1}$ and $(2d_{5/2})_\nu^{-1}(L=2)$, $(1g_{7/2})_\nu^{-1}(L=4)$, and $(1h_{11/2})_\nu^{-1}(L=5)$ states in ^{143}Sm, ^{141}Nd, ^{139}Ce, and ^{137}Ba nuclei. The ground state in all of these nuclei is assumed $\frac{3}{2}^+$ and containing the entire strength of the $(2d_{3/2})_\nu^{-1}$ state. The data for ^{143}Sm and ^{141}Nd were taken from Ref. 1.

the $N=81$ nuclei in Fig. 15, the exceptions being the $(3s_{1/2})_\nu^{-1}$ state in ^{139}Ce and the $(1h_{11/2})_\nu^{-1}$ states in ^{137}Ba and ^{139}Ce. In the former case the missing strength is probably due to our inability to identify all the $l=0$ transitions, as pointed out in Sec. III. In the case of the $(1h_{11/2})_\nu^{-1}$ states in ^{139}Ce and ^{137}Ba, there is also the additional possibility that the DWBA cross sections are perhaps very sensitive to small deviations from the best-fit optical-model parameters for these nuclei as we chose to use only the average fixed-geometry parameters of Refs. 5 and 6. As was shown in Paper I, the $(1h_{11/2})_\nu^{-1}$ DWBA calculations do exhibit an enhanced sensitivity to the extent of damping of the form factor in the nuclear interior.

V. CONCLUSIONS

The present paper completes the sequence of (p, d) measurements on $N=82$ nuclei to learn about the structure of neutron-hole states in the $50<N\leq 82$ region. Conclusions about the success of FRNL DWBA calculations and FRNL DWBA calculations including density-dependent corrections to the effective pn interaction were stated in Paper I. Similarly, results peculiar to nuclei discussed in Paper I are not summarized here. Conclusions of general validity for all nuclei in both papers and significant results pertinent to the present paper are presented below:

(i) No $2f$ or $3p$ states in the $82<N\leq 126$ major shell are observed with any measurable intensity in all four nuclei indicating that shell closure at $N=82$ is a good assumption.

(ii) For reasons discussed in Sec. III, only the ground-state $l=2$ transition was assigned $J^\pi=\frac{3}{2}^+$. This assignment leads to reasonable values of the summed strengths for both the $(2d_{3/2})_\nu^{-1}$ and $(2d_{5/2})_\nu^{-1}$ states.

(iii) Considerable splitting of the $(2d_{5/2})_\nu^{-1}$ and $(1g_{7/2})_\nu^{-1}$ states is observed. The lower four components of the $(2d_{5/2})_\nu^{-1}$ state show identifiable systematic trends with changing Z.

(iv) At least two components are observed for both the $(1h_{11/2})_\nu^{-1}$ and the $(3s_{1/2})_\nu^{-1}$ states, with the lower component carrying most of the single-hole strength.

(v) The relative spacing of single-neutron-hole states decreases as one goes from ^{137}Ba to ^{143}Sm. This can be qualitatively understood in terms of the pn interaction between the neutron and the valence protons that are filling the same shell-model orbits as the neutrons in the $50<N\leq 82$ range.

(vi) There seems to be a loss of $(1h_{11/2})_\nu^{-1}$ strength in ^{139}Ce and ^{137}Ba as compared to the values of this strength in ^{143}Sm and ^{141}Nd. A similar situation exists for the $(3s_{1/2})_\nu^{-1}$ strength in ^{139}Ce, probably due to our inability to identify all the components of the $(3s_{1/2})_\nu^{-1}$ state. Apart from these special cases, the summed spectroscopic strengths for the various neutron-hole states agree among all the nuclei to better than 20%.

ACKNOWLEDGMENTS

The authors gratefully acknowledge the assistance of Dr. G. F. Trentelman in accumulating the data. Helpful discussions with Dr. K. Kolltveit and Dr. J. Borysowicz are sincerely appreciated.

---

†Work supported by the National Science Foundation.

[1]R. K. Jolly and E. Kashy, Phys. Rev. C 3, 887 (1971).
[2]K. Yagi, Phys. Letters 28B, 455 (1969).
[3]C. Maples, G. W. Goth, and J. Cerny, University of California Radiation Laboratory Report No. UCRL 16964, 1966 (unpublished).
[4]R. H. Bassel, R. M. Drisko, and G. R. Satchler, Oak Ridge National Laboratory Report No. ORNL 3240 (unpublished); and a subsequent ORNL memorandum to users of JULIE, 1966 (unpublished).
[5]F. G. Perey, Phys. Rev. 131, 745 (1963).
[6]C. M. Perey and F. G. Perey, Phys. Rev. 132, 755 (1963).
[7]F. G. Perey and D. S. Saxon, Phys. Letters 10, 107 (1964).
[8]F. G. Perey, in *Proceedings of the Rutherford Jubilee International Conference, Manchester, England, 1961*, edited by J. B. Birks (Heywood and Company, Ltd., London, England, 1962), p. 125.
[9]J. B. French and M. H. Macfarlane, Nucl. Phys. 26, 168 (1961).
[10]C. M. Lederer, J. M. Hollander, and I. Perlman, *Table of Isotopes* (John Wiley & Sons, Inc., New York, 1967), 6th ed.
[11]W. C. Parkinson, D. L. Henrie, H. H. Duhm, J. Mahoney, J. Saudinos, and G. R. Satchler, Phys. Rev. 178, 1976 (1969); S. Hinds, R. Middleton, J. H. Bjerregaard, O. Hansen, and O. Nathan, Nucl. Phys. 83, 17 (1966).
[12]K. Yagi, T. Ishimatsu, Y. Ishizaki, and Y. Sagi, Nucl. Phys. A121, 161 (1968).
[13]R. H. Fulmer, A. L. McCarthy, and B. L. Cohen, Phys. Rev. 128, 1302 (1962).
[14]G. Bruge, A. Chanmeaux, Ha Duc Long, and J. Picard, Centre d'Études Nucléaires de Saclay Progress Report, October 1968–September 1969 (unpublished).
[15]M. Kawai, K. Kubo, and H. Yamaura, Institute for Nuclear Study, University of Tokyo, Report No. PT-9, 1965 (unpublished).
[16]B. H. Wildenthal, E. Newman, and R. L. Auble, Phys. Rev. C 3, 1199 (1971).
[17]D. Von Ehrenstein, G. C. Morrison, J. A. Nolen, Jr., and N. Williams, Phys. Rev. C 1, 2066 (1970).
[18]R. K. Jolly and C. F. Moore, Phys. Rev. 145, 918 (1966); H. Christensen, B. Herskind, R. R. Borchers, and L. Westgaard, Nucl. Phys. A102, 481 (1967).